# Characterization of Deoxyribozymes That Synthesize Branched RNA†

Yangming Wang‡ and Scott K. Silverman*

*Department of Chemistry, University of Illinois at Urbana-Champaign, 600 South Mathews Avenue, Urbana, Illinois 61801*

*Received September 3, 2003; Revised Manuscript Received October 27, 2003*

ABSTRACT: We recently reported deoxyribozymes (DNA enzymes) that synthesize 2′,5′-branched RNA. The in vitro-selected 9F7 and 9F21 deoxyribozymes mediate reaction of a branch-site adenosine 2′-hydroxyl on one RNA substrate with the 5′-triphosphate of another RNA substrate. Here we characterize these DNA enzymes with respect to their branch-forming activity. Both 9F7 and 9F21 are much more active with $Mn^{2+}$ than with $Mg^{2+}$. The $K_{d,app}(Mg^{2+}) > 400$ mM but $K_{d,app}(Mn^{2+}) \approx 20-50$ mM, and the ligation rates $k_{obs}$ are orders of magnitude faster with $Mn^{2+}$ than with $Mg^{2+}$ (e.g., 9F7 $\sim 0.3$ $min^{-1}$ with 20 mM $Mn^{2+}$ versus 0.4 $h^{-1}$ with 100 mM $Mg^{2+}$, both at pH 7.5 and 37 °C). Of the other tested transition metal ions $Zn^{2+}$, $Ni^{2+}$, $Co^{2+}$, and $Cd^{2+}$, only $Co^{2+}$ supports a trace amount of activity. 9F7 is more tolerant than 9F21 of varying the RNA substrate sequences. For the RNA substrate that donates the adenosine 2′-hydroxyl, 9F7 requires YUA, where Y = pyrimidine and A is the branch site. The 3′-tail emerging from the branch-site A may have indefinite length, but it must be at least one nucleotide long for high activity. The 5′-triphosphate RNA substrate requires several additional nucleotides with varying sequence requirements (5′-pppGRMWR). Outside of these regions that flank the ligation site, 9F7 and 9F21 tolerate any RNA substrate sequences via Watson−Crick covariation of the DNA binding arms that interact directly with the substrates. 9F7 provides a high yield of 2′,5′-branched RNA on the preparative nanomole scale. The ligation reaction is effectively irreversible; the pyrophosphate leaving group in the ligation reaction does not induce 2′,5′-cleavage, and pyrophosphate does not significantly inhibit ligation except in 1000-fold excess. Deleting a specific nucleotide in one of the DNA binding arms near the ligation junction enhances ligation activity, suggesting an interesting structure near this region of the deoxyribozyme−substrate complex. These data support the utility of deoxyribozymes in creating synthetic 2′,5′-branched RNAs for investigations of group II intron splicing, debranching enzyme (Dbr) activity, and other biochemical reactions.

Many new deoxyribozymes (DNA enzymes) with interesting catalytic activities have been discovered using in vitro selection (*1*−*5*). Our laboratory has recently focused on identifying and characterizing deoxyribozymes that ligate RNA (*6*−*8*). Some of our most intriguing DNA enzymes ligate a specific internal RNA 2′-hydroxyl group with a 5′-triphosphate, forming a 2′,5′-branched RNA (Figure 1A) (*9*). In this report, we provide detailed characterization of the RNA branch-forming reactions mediated by 9F7 and 9F21, two deoxyribozymes that use a specific adenosine 2′-hydroxyl as the branch-site nucleophile (*9*). RNA molecules with 2′,5′-branches are formed naturally by the spliceosome (*10*) and by group II introns during self-splicing (*11*−*13*). For spliced mRNAs, the branch-site nucleotide is invariably adenosine in yeast and usually adenosine in other cases (*10*). Similarly, in group II introns, the branch site is almost always adenosine (*14*, *15*). We therefore anticipate that 9F7, 9F21, and other deoxyribozymes that will be discovered by ongoing selection experiments will be useful for preparing synthetic 2′,5′-branched RNAs that are directly relevant to biochemical processes such as RNA splicing and lariat degradation by debranching enzyme Dbr[1] (*16*, *17*). In this report, we provide detailed characterization of the 9F7 and 9F21 branch-forming activities.

## EXPERIMENTAL PROCEDURES

*RNA Substrates and Deoxyribozymes.* The left-hand RNA substrate (L) is of minimal sequence 5′-UAAUACGACUCACUAUA-3′. In many cases, the 3′-terminal nucleotide is C instead of A; the particular sequence is noted for each experiment. Variants of this sequence were prepared either by solid-phase synthesis (Dharmacon, Inc., Lafayette, CO, or HHMI−Keck Laboratory, Yale University) or by in vitro transcription using T7 RNA polymerase with an appropriate double-stranded DNA template (*43*). This template was

† This research was supported by the Burroughs Wellcome Fund (New Investigator Award in the Basic Pharmacological Sciences), the March of Dimes Birth Defects Foundation (Research Grant 5-FY02-271), the National Institutes of Health (Grant GM-65966), the Petroleum Research Fund, administered by the American Chemical Society (38803-G4), and the UIUC Department of Chemistry (all to S.K.S.). S.K.S. is the recipient of a fellowship from the David and Lucile Packard Foundation.

* Corresponding author. Phone: (217) 244-4489. Fax: (217) 244-8024. E-mail: scott@scs.uiuc.edu.

‡ Department of Biochemistry, University of Illinois.

[1] Abbreviations: Dbr, lariat debranching enzyme; $k_{obs}$, observed rate constant; $K_{d,app}$, apparent dissociation constant; MALDI, matrix-assisted laser desorption/ionization; $PP_i$, pyrophosphate; $k_{bkgd}$, background rate constant; HEPES, 4-(2-hydroxyethyl)piperazine-1-ethanesulfonic acid; EDTA, ethylenediaminetetraacetic acid.

10.1021/bi0355847 CCC: $25.00 
Published on Web 12/02/2003

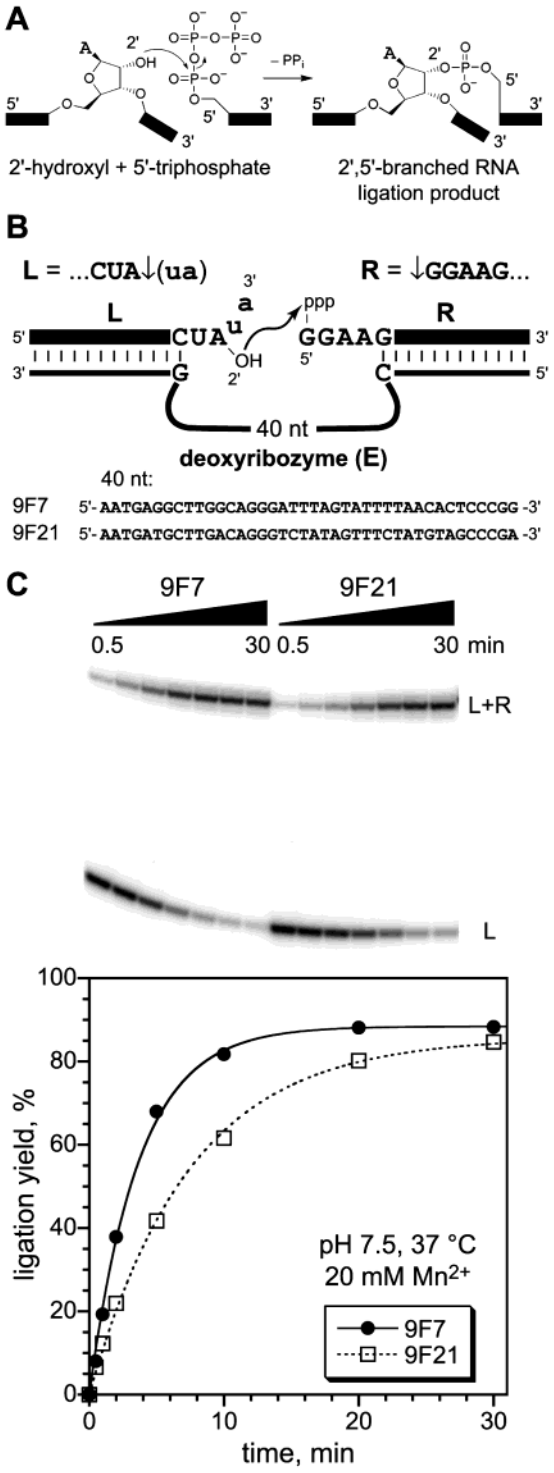


FIGURE 1: Ligation reaction to form 2′,5′-branched RNA as mediated by the 9F7 and 9F21 deoxyribozymes. (A) Chemical reaction between the branch-site adenosine 2′-hydroxyl and the 5′-triphosphate guanosine. Data demonstrating the structural assignment of the ligation product as a 2′,5′-branched RNA were included in our preliminary communication (*9*). (B) Intermolecular format for the ligation reaction. For small-scale kinetic assays, either the left-hand RNA substrate (L) or the right-hand substrate (R) is $^{32}$P-radiolabeled. Shown are the 40-nt enzyme region sequences of 9F7 and 9F21. Note the compact nomenclature used to denote the sequences of L and R. (C) Typical ligation assays and kinetic data. Assays were performed in 50 mM HEPES, pH 7.5, 150 mM NaCl, 2 mM KCl, and 20 mM $MnCl_2$ at 37 °C with 5′-$^{32}$P-radiolabeled L substrate. The sequence of L was ...UA↓(uc) prepared by solid-phase synthesis (see Experimental Procedures). $k_{obs}$ values: 9F7, 0.27 min$^{-1}$; 9F21, 0.13 min$^{-1}$.

prepared either by annealing two synthetic DNA oligonucleotides (for transcripts that terminate in a 2′,3′-diol) or by PCR (for templates that terminate with an encoded HDV ribozyme and therefore transcripts that terminate with a 2′,3′-cyclic phosphate). All transcripts included a leading 5′-GGA... in addition to the sequence above, to permit use of T7 RNA polymerase. The right-hand RNA substrate (R) is of minimal sequence 5′-GGAAGAGAUGGCGACGG-3′, prepared by transcription from annealed oligonucleotide templates. These sequences of L and R correspond to those used during the selection procedure that led to the discovery of 9F7 and 9F21 (*6*, *9*). Each deoxyribozyme (E) is of sequence 5′-*CCGTCGCCATCTC*-$N_{40}$-*GTGAGTCGTATTA*TCC-3′, where $N_{40}$ is the enzyme region; see the specific 9F7 and 9F21 sequences in Figure 1B. For the NUA↓(ua) and ↓GGAAN experiments in Figures 4 and 5, the appropriate single-underlined DNA nucleotide in the deoxyribozyme was changed to the Watson−Crick complement. For the comprehensive binding arm experiments in Figure 6, the entire DNA binding arms (italics) were changed to complement the RNA substrates. The boldface underlined G nucleotide in the left-hand DNA binding arm is deleted in all of the 9F7 deoxyribozymes in this report, as explained in Figure 11; the RNA nucleotide opposite this position in the left-hand RNA substrate is left unpaired. Note that the DNA binding arm with the deleted nucleotide is termed the left-hand (not the right-hand) DNA binding arm, because it binds to the left-hand RNA substrate. The analogous DNA nucleotide of 9F21's left-hand DNA binding arm was *not* deleted except for the specific experiment shown in Figure 11. DNA oligonucleotides were obtained from IDT (Coralville, IA). All DNA and RNA oligonucleotides were purified by 8%, 12%, or 20% denaturing PAGE as appropriate, with running buffer 1× TBE (89 mM each Tris and boric acid, 2 mM EDTA, pH 8.3).

*Kinetics Assays.* The kinetics assays used the trimolecular format shown in Figure 1B. The $^{32}$P-radiolabeled left-hand RNA substrate L was the limiting reagent relative to the right-hand substrate R and deoxyribozyme E. The ratio L:E:R was ~1:3:6 to 1:10:30, with the concentration of E equal to ~0.5−3 $\mu$M. Alternatively, R was radiolabeled and the limiting reagent, with equivalent results. Increasing the concentration of E or R (or both) did not significantly change the observed kinetics or yields, indicating that the observed yields were not limited by availability of E or R (data not shown). See our laboratory's previous report for details of the annealing and reaction procedure (*6*). In all cases, values of $k_{obs}$ and final yield were obtained by fitting the yield versus time data directly to first-order kinetics; i.e., yield (%) = $100 \times Y(1 - e^{-kt})$, where $k = k_{obs}$ and $Y$ = final yield in %. In all of the curve fits, the data clearly level off at a final yield less than 100%, indicating that the fitted value of $Y$ is meaningful. However, in many cases in this report, the final yield was >85%.

*Assays with Varied Substrate Sequences.* For the assays in which the L sequence was varied (first rows of panels A and B in Figure 4), L was prepared by transcription terminating with a 2′,3′-cyclic phosphate for NUA↓(ua), CUA↓(na), and CUA↓(un) or by transcription terminating with a 2′,3′-diol for CNA↓(ua) and CUN↓(ua). For the assays in which R was varied (second rows of panels A and B in Figure 4, as well as Figure 5), L was prepared by solid-

phase synthesis for all assays except ↓GGAAN, for which L was prepared by transcription terminating in a 2′,3′-diol. When L was varied, $^{32}$P-radiolabeled R was prepared by transcription with [α-$^{32}$P]CTP and was the limiting reagent in the trimolecular assay. When R was varied, $^{32}$P-radiolabeled L was prepared either by 5′-labeling with T4 polynucleotide kinase and [γ-$^{32}$P]ATP or by internal radiolabeling with [α-$^{32}$P]CTP during transcription and was the limiting reagent in the trimolecular assay.

*Preparative Application of 9F7 To Create 2′,5′-Branched RNA.* The preparative ligation reaction shown in Figure 9 was performed as follows. A sample containing 2.0 nmol of left-hand substrate L [sequence ...UA↓(uc) prepared by solid-phase synthesis], 2.2 nmol of 9F7 deoxyribozyme E, and 2.4 nmol of right-hand substrate R in 120 μL of 5 mM HEPES, pH 7.5, 15 mM NaCl, and 0.1 mM EDTA was annealed by heating at 95 °C for 4 min then cooling on ice for 5 min. The volume was increased to 200 μL containing 50 mM HEPES, pH 7.5, 150 mM NaCl, 2 mM KCl, and 20 mM $MnCl_2$; the $Mn^{2+}$ was added from a 100 mM aqueous stock. The 200 μL solution was incubated at 37 °C for 30 min and then mixed with an equal volume of low-dye stop solution (80% formamide, 1× TB, 50 mM EDTA, 0.0025% each bromophenol blue and xylene cyanol; this is a 10-fold lower concentration of each dye than is used for analytical samples). The sample was electrophoresed on a 3 mm thick 20% denaturing polyacrylamide gel (7 M urea) in a single 5 cm wide lane. The running buffer was 1× TBE. The bands corresponding to the product (L + R), the deoxyribozyme (E), and the unreacted left-hand substrate (L) were visualized by UV shadowing and separately excised with razor blades. After manual crushing with a glass rod, the nucleic acids were extracted with two portions of TEN (10 mM Tris, pH 8.0, 1 mM EDTA, 300 mM NaCl) totalling 10 mL of eluted volume; this required 12−13 mL of added TEN, of which 2−3 mL remained soaked into the polyacrylamide pellet and was unrecoverable. For each extraction, the sample containing polyacrylamide and TEN was placed on a nutator at 4 °C for several hours, centrifuged at ≥1000 rpm for ≥10 min, and filtered through a 0.45 μM syringe filter. To the combined elutions for each product was added 27 mL of cold ethanol, and the sample was placed at −20 °C for at least 6 h. The nucleic acids were precipitated by centrifugation at 8000 rpm (∼10000*g*) for 30 min at 4 °C (Beckman JS-13.1 rotor), washed with 1 mL of cold 75% ethanol, dissolved in 300 μL of water, and quantitated by UV absorbance ($A_{260}$); yields are listed in the Figure 9 caption. MALDI mass spectra of the ligation product and linear standard RNA were obtained in the Mass Spectrometry Laboratory of the UIUC School of Chemical Sciences.

## RESULTS

*Establishing Optimal Incubation Conditions for 2′,5′-Branch Formation by 9F7 and 9F21.* We previously communicated the selection procedure used to identify the 9F7 and 9F21 deoxyribozymes (*9*). These DNA enzymes each have a 40-nucleotide "enzyme region", and they ligate two RNA substrates in a trimolecular format (Figure 1B). Although both $Mg^{2+}$ and $Mn^{2+}$ support ligation activity, the ligation rates ($k_{obs}$) are considerably faster with $Mn^{2+}$ (Figure 1C). The complete $Mg^{2+}$ and $Mn^{2+}$ dependencies for each DNA enzyme at pH 7.5 and 37 °C are shown in Figure 2.

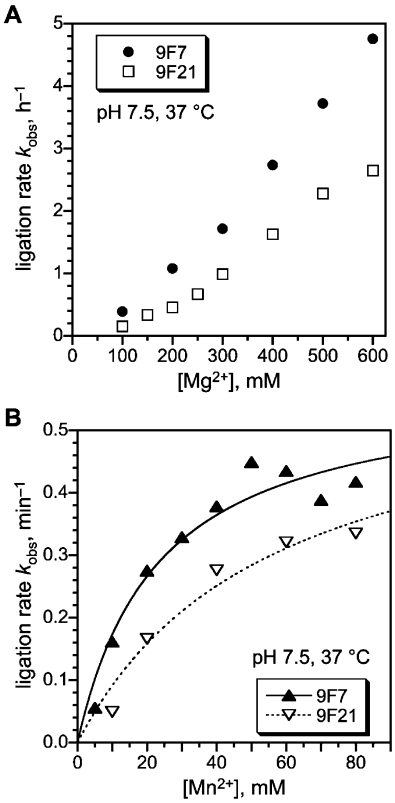


FIGURE 2: Dependence of 9F7 and 9F21 ligation activity on $Mg^{2+}$ and $Mn^{2+}$ concentration. (A) $Mg^{2+}$ dependence. (B) $Mn^{2+}$ dependence. The fit values of $K_{d,app}(Mn^{2+})$ are 23 ± 7 mM for 9F7 and 56 ± 28 mM for 9F21. The fit equation is $k_{obs} = k_{max}[Mn^{2+}]/([Mn^{2+}] + K_{d,app})$; $k_{max}$ fits to ∼0.6 min$^{-1}$ in both cases. Assays were performed in 50 mM HEPES, pH 7.5, 150 mM NaCl, 2 mM KCl, and the indicated concentration of $MgCl_2$ or $MnCl_2$ at 37 °C. Concentrations of $Mn^{2+}$ ≥80 mM led to considerable inhibition of ligation. For example, at 150 mM $Mn^{2+}$ the 9F7 ligation yield was only 10−20% after 30 min versus 91% for 20 mM $Mn^{2+}$. The left-hand substrate for the $Mg^{2+}$ experiments was ...UA↓(ua) prepared by transcription terminating with a 2′,3′-diol. The left-hand substrate for the $Mn^{2+}$ experiments was ...UA↓(uc) prepared by solid-phase synthesis.

Neither 9F7 nor 9F21 has reached its maximal $k_{obs}$ even at 600 mM $Mg^{2+}$; indeed, the $k_{obs}$ versus [$Mg^{2+}$] data have not yet begun to turn over at this concentration (Figure 2A). We conservatively estimate that $K_{d,app}(Mg^{2+})$ is >400 mM for both deoxyribozymes. In contrast, $Mn^{2+}$ is much more efficient at supporting branch formation; $K_{d,app}(Mn^{2+})$ is ≪100 mM for both DNA enzymes (Figure 2B). The $Mn^{2+}$ experiments are hindered by the tendency of high $Mn^{2+}$ concentrations (80−200 mM) to inhibit the ligation reaction considerably (see Figure 2 caption).

Several other transition metal ions were tested for their ability to support ligation. Neither $Zn^{2+}$, $Ni^{2+}$, nor $Cd^{2+}$ is a cofactor for 9F7 or 9F21 between 10 μM and 10 mM (see Supporting Information). However, $Co^{2+}$ does support a barely detectable amount of ligation activity at high concentrations. The estimated $k_{obs}$ is only ∼4 × 10$^{-6}$ min$^{-1}$ at 10 mM $Co^{2+}$, which is about 10$^5$-fold lower than the $k_{obs}$ with 20 mM $Mn^{2+}$ (∼0.3 min$^{-1}$). The assays with each of the divalent metal ions were performed in buffers containing 150 mM NaCl and 2 mM KCl, which were the salt conditions used during the selection procedure. Independently varying [NaCl] from 0 to 300 mM and [KCl] from 0 to 100 mM with 20 mM $Mn^{2+}$ had no effect on the ligation rate or yield

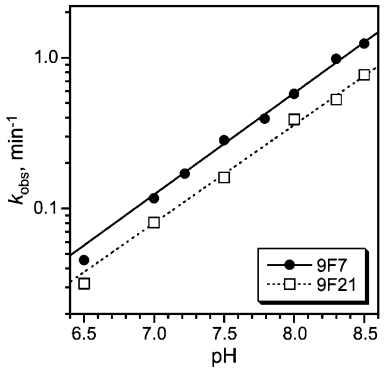


FIGURE 3: pH dependence of the ligation rate $k_{obs}$ for 9F7 and 9F21. Assays were performed in 50 mM buffer, 150 mM NaCl, 2 mM KCl, and 20 mM $MnCl_2$ at 37 °C. The buffer compound was PIPES (pH 6.5), HEPES (pH 7.0−7.8), or EPPS (pH 8.0−8.5). Data acquired at higher pH (8.8−9.0 with CHES) were discarded due to obvious $Mn^{2+}$ oxidation (development of brown color in the reaction solution). The fit lines have slopes of 0.71 (9F7) and 0.68 (9F21). The left-hand substrate was ...UA↓(uc) prepared by solid-phase synthesis.

of 9F7 or 9F21 (data not shown). Therefore, these deoxyribozymes do not require monovalent metal ions for their activity.

We examined the pH dependence of branched RNA formation for both 9F7 and 9F21 (Figure 3). Between pH 6.5 and pH 8.5 at 37 °C, a plot of $k_{obs}$ (in 20 mM $Mn^{2+}$) versus pH is log-linear with a slope of just under 1. This is commonly observed for nucleic acid enzymes (*18*−*26*) and indicates that the reaction involves net removal of one proton.

*Branch Formation Depends on the RNA Substrate Sequence near the Ligation Site.* Using a systematic series of RNA substrates and (where appropriate) mutated deoxyribozymes, we determined the extent to which 9F7 and 9F21 can ligate RNAs of varying sequence. To simplify the presentation of these data, we use the following nomenclature convention for the RNA substrates (Figure 1B). The left-hand RNA substrate that donates the branch-site adenosine is written in the 5′-to-3′ direction as (for example) ...CUA↓(ua). The arrow denotes the 2′−5′ ligation site, i.e., the reaction site of the 2′-hydroxyl of the left-hand substrate's A↓ nucleotide with the right-hand substrate's 5′-triphosphate G. The A↓ nucleotide is the branch-site adenosine, and the lowercase nucleotides in parentheses constitute the 3′-tail. Similarly, the right-hand RNA substrate is ↓GGAAG..., where the ↓G nucleotide bears the 5′-triphosphate that is attacked by the 2′-hydroxyl on the left-hand substrate's A↓ nucleotide. Specific nucleotide positions are underlined for emphasis when warranted. The arbitrary RNA substrates used during the selection procedure itself for 9F7 and 9F21 were ...CUA↓(uc) and ↓GGAAG... for the left-hand and right-hand RNA substrates, respectively (*9*). Related selections that were performed simultaneously used a left-hand substrate of sequence ...CUA↓(ua) that differs only in the last nucleotide. This particular sequence was also used frequently in the assays described here.

We first examined the five left-hand RNA substrate nucleotides near the ligation junction, namely, each position of CUA↓(ua). Each of these nucleotides was changed separately to the other three standard RNA nucleotides, and the effects on ligation yield were assayed with both 9F7 and 9F21 (Figure 4). Because the first nucleotide CUA↓(ua) was originally Watson−Crick base-paired with a DNA nucleotide in the selection design (Figure 1B), we tested the RNA substrates modified at this position using deoxyribozymes for which the corresponding DNA nucleotide was mutated to maintain base pairing. The results clearly indicate that 9F7 requires only YUA↓(nn) for these five nucleotides (Y = pyrimidine), whereas 9F21 requires CUA↓(nn). In particular, any sequence of the two-nucleotide 3′-tail (nn) permits successful ligation.

For the four right-hand RNA substrate nucleotides ↓GGAAG, 9F7 is relatively tolerant to single mutations, because any nucleotides are acceptable at these positions with high ligation yield (Figure 4). For the ↓GGAAG position, again the corresponding DNA nucleotide was changed to maintain Watson−Crick base pairing. The first position (↓G) was not varied in these tests because the necessary 5′-triphosphate RNAs were unavailable; in vitro transcription was used to prepare the 5′-triphosphate G RNAs, and T7 RNA polymerase has a strict 5′-G requirement. 9F21 was significantly less tolerant than 9F7 at certain positions of ↓GGAAG (compare fourth and second rows of Figure 4).

The data in Figure 4 for mutations in ↓GGAAG are single time points at 2−4 h, whereas the original RNA substrates require only 20−30 min for maximal ligation (Figure 1C). We examined more comprehensively the time courses of 9F7 ligations with single nucleotide changes at each position of ↓GGAAG (Figure 5). The data reveal a relatively complicated yet clear sequence preference that may be summarized as ↓GRMWR, using the standard nucleotide abbreviations for which R = purine A or G, M = A or C, and W = A or U.

We examined the possibility that the requirement for YUA↓ in the left-hand RNA substrate may originate in a Watson−Crick interaction with a nucleotide in the deoxyribozyme's enzyme region. If this were true, then other RNA nucleotides would be tolerated at this position via appropriate covariation of the DNA. We noted that the 3′-most nucleotide of the enzyme region (i.e., the nucleotide immediately prior to the binding arm of the DNA) is G in 9F7 and A in 9F21 (Figure 1B). It is conceivable that this nucleotide (G or A) forms either a wobble or canonical base pair with the YUA↓ nucleotide. To test this, we mutated the G in the 9F7 DNA to either A or T. If a base pair exists between the corresponding DNA and RNA nucleotides, the G/A-U combinations of DNA−RNA should have high ligation yields, whereas the T-U combination should have a poor yield. However, all of the combinations maintained high yields (see Supporting Information), indicating that this particular DNA nucleotide is *not* interacting with the RNA via simple base pairing. When the RNA substrate is mutated to YAA↓, we already determined that the ligation yield decreases sharply (Figure 4A, second panel of first row). If a base pair between this RNA position and the DNA were present for the YUA↓ substrate, then a compensatory DNA mutation from G → T would restore base pairing for the YAA↓ mutant substrate and thus restore high ligation activity. However, the ligation yield remained very low (see Supporting Information), again indicating that this specific DNA nucleotide does not interact with the RNA substrate via a base pair.

Finally, we considered the possibility that the 9F7 left-hand substrate requirement for YUA↓(nn) originates in the need for a particular DNA nucleotide at the corresponding

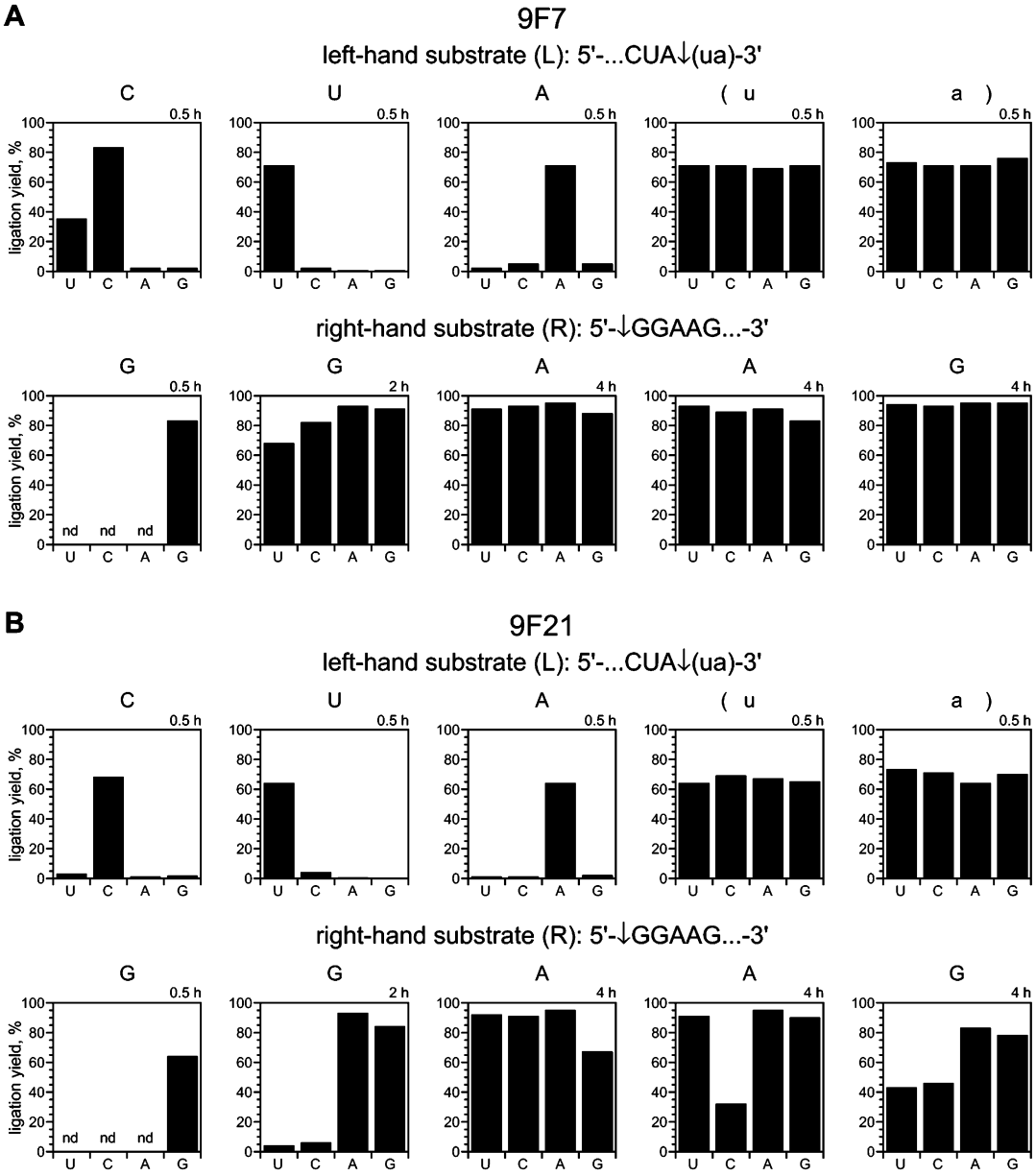


FIGURE 4: Survey of the ligation activities of 9F7 and 9F21 with RNA substrate sequences that vary near the ligation site. All assays were performed in 50 mM HEPES, pH 7.5, 150 mM NaCl, 2 mM KCl, and 20 mM $MnCl_2$ at 37 °C. (A) 9F7, with systematic changes to the left-hand RNA substrate nucleotides CUA↓(ua) and right-hand RNA substrate nucleotides ↓GGAAG. (B) 9F21, with changes to the same nucleotides. See Experimental Procedures for preparation of substrates. The time points at which the data were collected in the individual experiment are shown above each plot. For complete time courses for 9F7 and the ↓GGAAG nucleotides, see Figure 5. For longer time points for variations at the first three nucleotides, CUA↓, of the L substrate, see Supporting Information. At the key branch-site nucleotide CUA↓(nn), 9F7 ligates C with 45% yield in 8 h and both U and G with ~20% yield in 8 h. For changes at the CUA↓(ua) and ↓GGAAG positions of the RNA, the corresponding DNA binding arm nucleotides were changed to maintain Watson−Crick complementarity (Figure 1B; see text for details).

position in the deoxyribozyme, rather than a requirement for a Watson−Crick base pair. That is, perhaps 9F7 merely requires a purine at the corresponding DNA position, and the Y requirement in the RNA is a consequence and not a cause. To check this, we tested all combinations of NUA↓(ua) with all four possible 9F7 deoxyribozymes. For each of the four RNA substrates, there is one Watson−Crick DNA match and three mismatches, requiring 16 assays in all. The Watson−Crick match was universally accepted with high ligation yield, whereas mismatches generally reduced the yield (see Supporting Information). A similar observation was made for the ↓GGAAN position in the RNA. Thus these two nucleotide positions mark the boundaries at which Watson−Crick base pairing begins for each binding arm (Figure 1B).

*Branch Formation Does Not Depend on the RNA Substrate Sequence Far from the Ligation Site*. The independence of ligation activity on RNA sequence far from the ligation site was confirmed by examining multiple modifications to the RNA substrate sequences (Figure 6). In several parallel experiments, *all* of the nucleotides in the RNA binding arms were systematically changed, and the corresponding DNA nucleotides were altered to maintain base pairing. In a strategy similar to that applied previously to a different deoxyribozyme (*8*), merely four combinations of RNA substrates and 9F7 deoxyribozymes were sufficient to examine

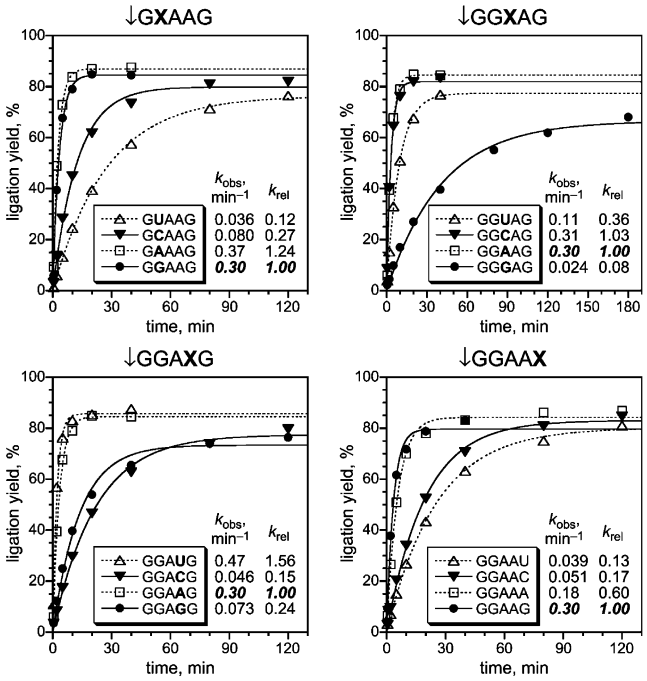


FIGURE 5: Detailed kinetics for 9F7 with right-hand RNA substrates varying at the ↓GGAAG positions. All assays were performed in 50 mM HEPES, pH 7.5, 150 mM NaCl, 2 mM KCl, and 20 mM $MnCl_2$ at 37 °C.

comprehensively the binding arms (Figure 6). These results clearly demonstrate that 9F7 operates via the simple binding arm strategy shown in Figure 1B. The 9F21 DNA enzyme showed more variation in $k_{obs}$ and yield than 9F7 when the substrate sequences were systematically changed in the same way, but the 9F21 ligation yield after 60 min with 20 mM $Mn^{2+}$ was always >60% regardless of binding arm sequence.

*Variations in 3′-Tail Length Are Accepted.* The experiments described above establish the minimal requirements for the RNA nucleotides that span the ligation junction and extend along the DNA binding arms. To complete the survey of RNA substrate sequence dependence for 9F7 and 9F21, we tested the ability of the deoxyribozymes to function with varying lengths of 3′-tail extending from the branch-site adenosine. These 3′-tail nucleotides are at the 3′-end of the left-hand RNA substrate, so these assays used left-hand RNA substrates of varying length. These are written as UA↓(*n*...), where the (*n*...) part has length from 0 to 20 nucleotides in the assays performed here.

We first examined shorter tails than the two-nucleotide (ua) tails shown in Figure 4. A tail length of zero means that there are zero nucleotides to the 3′-side of the adenosine that donates the 2′-hydroxyl. For such substrates, if the deoxyribozymes use the same nucleophilic branch-site adenosine 2′-hydroxyl as for a nonzero tail-length substrate, then the ligation product will be linear 2′−5′-linked RNA. As expected, both 9F7 and 9F21 indeed create linear 2′−5′ RNA from "tail-less" UA↓ substrates (Figure 7A). The ligation rates were diminished ~100-fold relative to that for forming a true 2′,5′ branch (Figure 7B,C); 9F7 has $k_{obs}$ ~0.1−0.2 $h^{-1}$ for linear 2′−5′ RNA ligation at 20 mM $Mn^{2+}$, and 9F21 is about 2-fold slower than 9F7. However, significant yields were still observed on a reasonable time scale (e.g., >50% yield in 6 h for 9F7). Furthermore, the products are linear, as evidenced by the absence of a gap in their partial alkaline hydrolysis ladders (Figure 7D). As detailed in the Supporting Information, the 2′−5′ (rather than 3′−5′) nature of these ligation products was demonstrated via a combination of partial alkaline hydrolysis and relatively high reactivity of the 2′−5′ linkages to hydrolytic cleavage, as previously described (*6*).

With a short one-nucleotide 3′-tail, ligation activity was also maintained with little change in $k_{obs}$ (data not shown). However, the more interesting branched products would likely be those with *longer* 3′-tails, because the branched intermediates of RNA splicing have tails that can be several hundred nucleotides in length, particularly when including portions of the 3′-exon. We chose two longer tail lengths for which the (*n*...) part of UA↓(*n*...) has length 8 or 20 nt, in addition to the 2-nt tail used during selection and in the assays of Figures 1−8. The 9F7 deoxyribozyme successfully ligates the longer tail substrates with high $k_{obs}$ and yield (Figure 8). The $k_{obs}$ only decreases 2-fold upon increasing the tail length from 2 to 20 nt, and the branch-site adenosine is maintained as described in our preliminary communication (*9*). These data strongly suggest that even longer 3′-tails will also be acceptable, although this remains to be tested explicitly. 9F21 also successfully ligated the longer left-hand substrates, although there was significant dimunition of activity relative to a 2-nt tail (e.g., ~40% ligation in 8 h with 20 mM $Mn^{2+}$ for both the 8-nt and 20-nt tail lengths with $k_{obs}$ ≈0.003 $min^{-1}$; see Supporting Information).

*Preparative Scale 2′,5′-Branched RNA Formation Using 9F7.* The 9F7 deoxyribozyme was employed to prepare 2′,5′-branched RNA on the nanomole scale (Figure 9). For this purpose, we used 9F7 along with the original RNA substrates used during the selection procedure itself, for which the ligation yield on the analytical scale is ≥85% (Figure 1C). A preparative ligation reaction was performed using 2.0 nmol of left-hand RNA substrate and a slight excess of deoxyribozyme (2.2 nmol) and right-hand RNA substrate (2.4 nmol) in a 200 μL reaction volume (10−12 μM each nucleic acid, none of which were radiolabeled). The reaction proceeded in 50% isolated yield *after* polyacrylamide gel electrophoresis, extraction, and precipitation. The recovery of deoxyribozyme was 77% of the amount originally used, which reflects losses during purification, and unreacted left-hand substrate was obtained in 15% yield. The final isolated yield of 2′,5′-branched RNA product in this case was 1.0 nmol.

As confirmation of structure, we obtained a MALDI mass spectrum of the 2′,5′-branched ligation product from the experiment in Figure 9. As expected, its molecular weight (10992 ± 11) was identical within experimental error to that of an isomeric linear standard RNA prepared independently by solid-phase synthesis with the same nucleotide composition (expected *m*/*z* 10985; found *m*/*z* 10986 ± 11).

*Attempted Application of 9F7 To Prepare Branched RNAs of Natural Sequence.* Deoxyribozyme-mediated formation of branched RNA would be most useful if *any* RNA substrates could be ligated. However, the above results indicate that 9F7 requires YUA↓(nn) on the left-hand substrate and ↓GRMWR on the right-hand substrate. Single-nucleotide differences in the right-hand substrate still provide high yields on an acceptable time scale (Figure 5), but "real" RNA sequences may have more than one difference. To test application of 9F7 for naturally occurring branched RNA

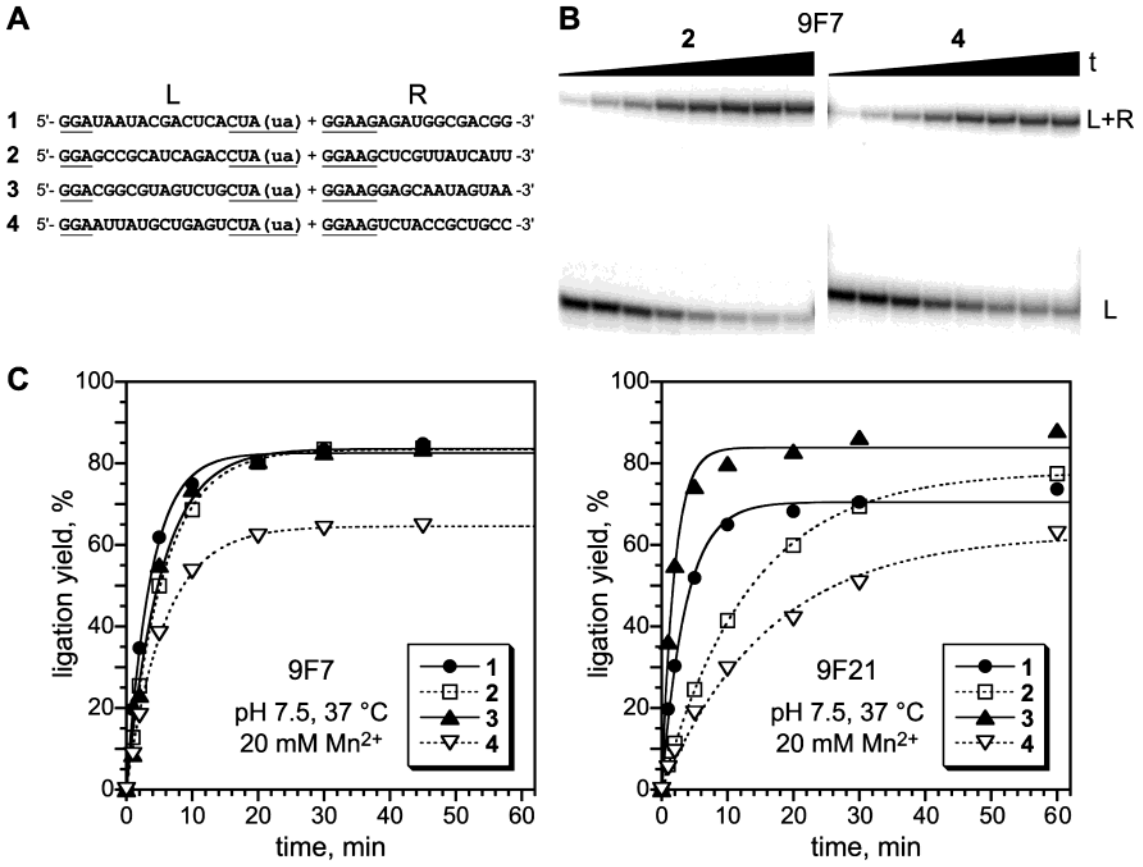


FIGURE 6: Survey of the ligation activities of 9F7 and 9F21 with RNA substrate sequences that vary away from the ligation site. (A) The four RNA substrate combinations, **1**−**4**. Nucleotides that are constant among all four sequences are underlined (the 5′-GGA is to permit transcription; the nucleotides nearer the ligation junction are investigated in Figures 4 and 5). As may be verified by looking vertically down each column of nonunderlined nucleotides, each of the four nucleotides, U, C, A, and G, is represented at every position in one of the four substrate combinations, **1**−**4**. For all RNA nucleotides within the substrate binding arms (see Figure 1B), the corresponding DNA nucleotide was the Watson−Crick complement, except in the 9F7 left-hand DNA binding arm, where one nucleotide was intentionally deleted as described in Figure 11. The left-hand substrates were prepared by transcription terminating with a 2′,3′-cyclic phosphate. (B) Representative PAGE images for substrates **2** and **4** assayed with 9F7. For a gel image for **1**, see Figure 1C, but note that the left-hand substrate in that figure has a different 3′-terminal nucleotide (C with a 2′,3′-diol in Figure 1C instead of A with a 2′,3′-cyclic phosphate here), so the $k_{obs}$ values are not identical. (C) Kinetic plots for all four substrate combinations for 9F7 (left) and 9F21 (right). $k_{obs}$ values for 9F7: **1**, 0.27 min$^{-1}$; **2**, 0.18 min$^{-1}$; **3**, 0.19 min$^{-1}$; **4**, 0.17 min$^{-1}$. $k_{obs}$ values for 9F21: **1**, 0.28 min$^{-1}$; **2**, 0.075 min$^{-1}$; **3**, 0.53 min$^{-1}$; **4**, 0.061 min$^{-1}$.

sequences, we examined branch formation with two sets of RNA substrates that form the branched core of two group II intron RNAs, the bI1 intron (*27*, *28*) and the ai5$\gamma$ intron (*29*−*32*). These are well-studied model systems for group II intron splicing (*33*, *34*). The bI1 branch junction is formed from ...CUA↓(UC...) + ↓GUGAG..., and the ai5$\gamma$ branch junction is ...CUA↓(UC...) + ↓GAGCG.... For bI1, there are two differences in the right-hand substrate compared with the 9F7 requirement (at positions ↓GUGAG), and for ai5$\gamma$, there are also two differences (↓GAGCG). Thus these two group II introns provide a stringent test of the extended applicability of 9F7. Unfortunately, in both cases, the ligation yield was <1% at 7 h under the same conditions of Figures 5 and 6 (data not shown). These results indicate that more than one nucleotide difference from the 9F7 requirement in the right-hand RNA substrate decreases the ligation activity to unacceptably low levels. Control experiments established that changing the RNA nucleotides far from the ligation site to the ai5$\gamma$ sequences led to no reduction in ligation yield (data not shown), consistent with the data in Figure 6. Therefore, it is solely the nucleotide differences near the ligation junction that are responsible for the variation in ligation yield.

*Irreversibility of the Ligation Reaction and Assaying Inhibition by Pyrophosphate.* In the ligation reaction (Figure 1A), a 2′-hydroxyl nucleophile attacks the 5′-triphosphate, forming a 2′,5′-branched linkage. The leaving group in this reaction is pyrophosphate ($PP_i$). Is this ligation reaction reversible or irreversible? To address this question, we incubated the 9F7 ligation products with $PP_i$ in the presence of the DNA enzyme. This is equivalent to testing the combination of the deoxyribozyme and $PP_i$ as a debranching reagent [the authentic debranching enzyme Dbr successfully debranches the product (*9*)]. No cleavage of the 2′,5′-branched linkage was detected in the presence of 9F7 with up to 1000 equivalents of $PP_i$ (0.5 mM $PP_i$; Figure 10A), indicating that the 9F7-mediated ligation reaction is effectively irreversible. We also examined the 9F7 ligation reaction (forward direction) in the presence of a 10−1000-fold excess of $PP_i$ (up to 0.5 mM). Inclusion of $PP_i$ did not detectably inhibit ligation except when a 1000-fold excess was used, and even then the reaction proceeded to an appreciable extent (Figure 10B).

*Effects of 2′-Deoxy Modifications near the Ligation Site.* We briefly examined the tolerance of 9F7 and 9F21 for

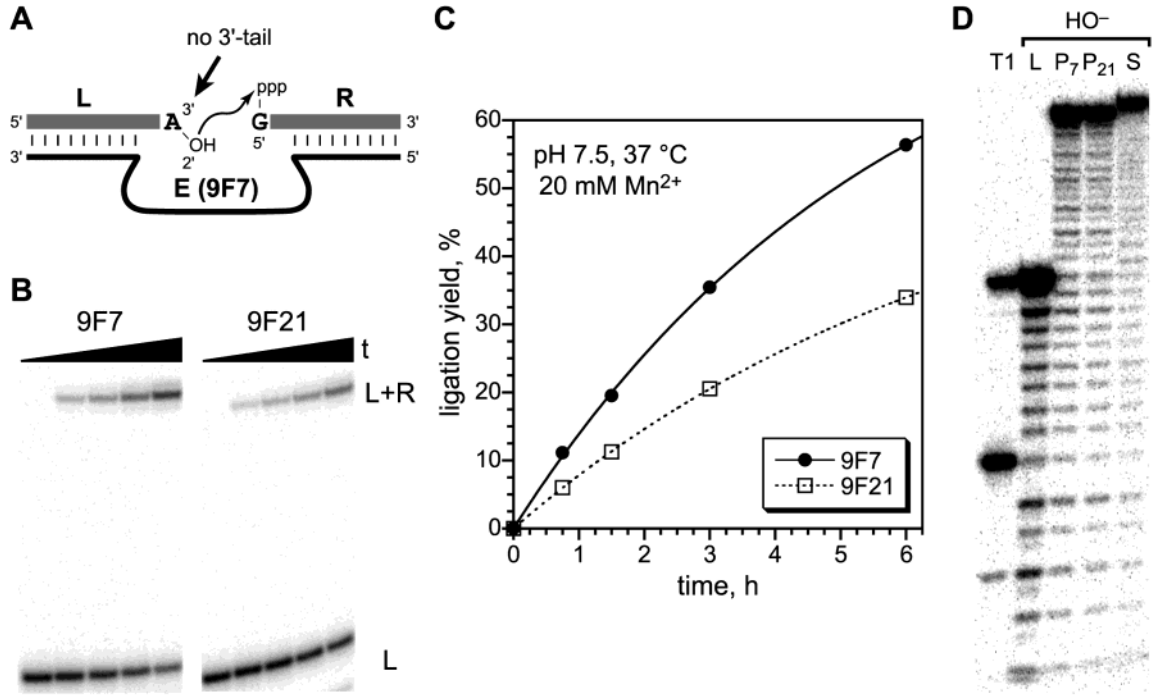


FIGURE 7: Determination of the tolerance of 9F7 and 9F21 to a tail-less left-hand substrate. (A) Diagram showing the ligation reaction with a tail-less left-hand RNA substrate. (B) PAGE images of the ligation reactions under conditions equivalent to those used in Figure 1C for the longer left-hand substrates. (C) Kinetics plots from the data in panel A. Fitting the first few data points to a straight line provides a rough estimate of the ligation rate $k_{obs}$ as 0.13 $h^{-1}$ (0.0022 $min^{-1}$) for 9F7 and 0.075 $h^{-1}$ (0.0013 $min^{-1}$) for 9F21. These values are ~100-fold lower than those for the 2-nt-tail substrate as shown in Figure 1C. Data points at >6 h incubation under these conditions are not feasible due to the onset of degradation (data not shown). (D) Partial alkaline hydrolysis demonstrates the linear nature of the ligation products. A gap is expected for a 2′,5′-branched product (*9*) but is not observed; see Supporting Information for data demonstrating that the 9F7 product is linked 2′−5′ and not 3′−5′. Conditions for partial alkaline hydrolysis: 50 mM $NaHCO_3$, 0.1 mM EDTA, 90 °C, 10 min; the pH at room temperature of the 50 mM $NaHCO_3$ solution was 9.2. Lane T1 is partial RNase T1 digestion of the 5′-$^{32}$P-radiolabeled tail-less left-hand RNA substrate standard, which allows ladder calibration (there is only one G within the left-hand substrate sequence; see Experimental Procedures). The remaining lanes are all partial alkaline hydrolysis of 5′-$^{32}$P-radiolabeled material, as follows: L, tail-less left-hand substrate UA↓ standard; P7, ligation product from 9F7 using this substrate; P21, product from 9F21; S, linear 3′−5′-linked standard of sequence UAUA↓GGAA (i.e., two nucleotides longer than the 9F7 and 9F21 products but identical in sequence and connectivity from the 5′-end to the branch-site adenosine). The S standard shows an identical pattern as $P_7$ and $P_{21}$ for all bands at or below the position of the L standard, as expected, whereas a slight difference is observed at the higher bands, also as expected (because of the extra two nucleotides within the linear portion of S).

2′-deoxynucleotides at all four positions of the left-hand substrate UA↓(ua) (data not shown). 9F7 tolerated a 2′-deoxy modification at any position of U<u>A</u>↓(<u>ua</u>) without significant decrease in yield. However, 9F21 functioned with a 2′-deoxy substitution only at UA↓(<u>ua</u>), although the U<u>A</u>↓(ua) 2′-deoxy substrate did show ~3% ligation. For both 9F7 and 9F21, no ligation was detected (<0.5%) when a 2′-deoxy modification was made at the branch-site A↓, as expected because the 2′-hydroxyl of that nucleotide is the required nucleophile in the ligation reaction.

*A Deleted Nucleotide Is Preferred in the DNA Binding Arm.* In the original sequence of the 9F7 clone (*9*), a deleted nucleotide was found in the left-hand DNA binding arm (i.e., the DNA that binds to the left-hand RNA substrate), as shown in Figure 11A. Originally, we presumed that this missing DNA nucleotide is an artifact due to the use of *Taq* polymerase during selection, and we intended simply to restore a nucleotide to this DNA position to maintain full Watson−Crick complementarity with the RNA substrate. However, when two 9F7 deoxyribozymes (one each with and without the missing nucleotide) were compared in 20 mM $Mn^{2+}$, the $k_{obs}$ was surprisingly 2-fold higher in the absence of the particular nucleotide (Figure 11B). The effect was even more pronounced in 80 mM $Mg^{2+}$, with an approximately 10-fold difference in $k_{obs}$ (data not shown). No such DNA deletion was found in the 9F21 sequence obtained directly from the selection procedure. When the deletion was made, the $k_{obs}$ again increased modestly (Figure 11C).

## DISCUSSION

The 9F7 and 9F21 are well-behaved DNA enzymes that ligate a specific adenosine 2′-hydroxyl to a 5′-triphosphate with formation of 2′,5′-branched RNA in high yield (Figure 1). Both deoxyribozymes prefer $Mn^{2+}$ over $Mg^{2+}$ (Figure 2), and the only other effective ion tested is $Co^{2+}$, which has $k_{obs}$ over 4 orders of magnitude lower than with $Mn^{2+}$. As is typical for catalytic nucleic acids, $k_{obs}$ increases linearly with pH (Figure 3); the slope indicates that a net total of one proton must be removed in the reaction. Through comprehensive RNA substrate dependence assays, the 9F7 deoxyribozyme is revealed to be useful for synthesis of 2′,5′-branched RNA with sequence requirements as summarized in Figure 12. The 9F7 requirements are YUA↓ on the left-hand substrate and ↓GRMWR on the right-hand substrate (Figures 5 and 6). In the right-hand substrate, the indicated nucleotides are preferred, although significant ligation rates and yields are maintained with any one mutation (two or more mutations are not tolerated). Any Watson−Crick bases

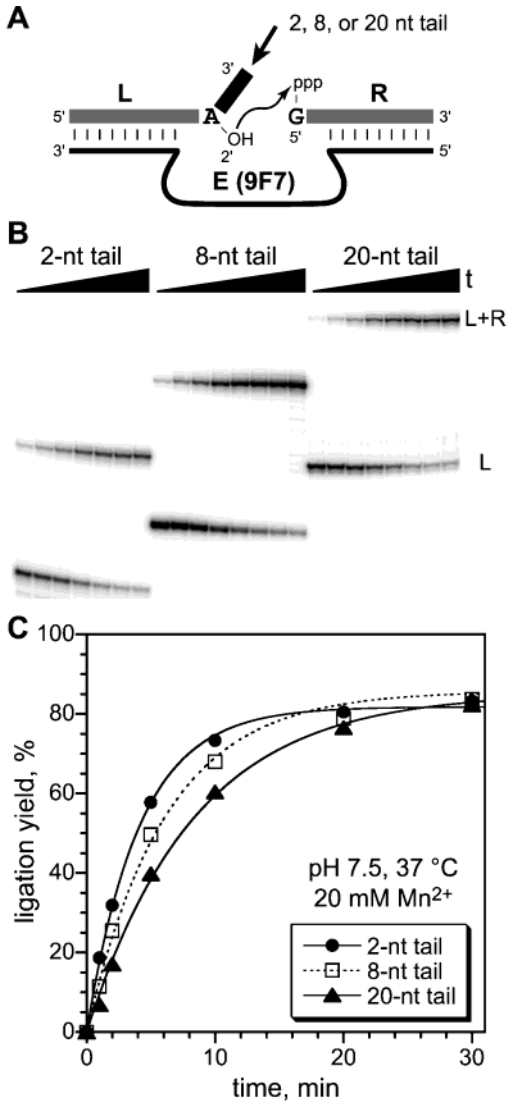


FIGURE 8: Determination of the 3′-tail-length dependence of 9F7 for longer tails. (A) Diagram highlighting the 3′-tail of the left-hand substrate. (B) Gel image for 9F7 kinetic experiments with tail lengths of 2, 8, or 20 nt. The incubation conditions were 50 mM HEPES, pH 7.5, 150 mM NaCl, 2 mM KCl, and 20 mM $MnCl_2$ at 37 °C. The three L substrate sequences were ...CUA↓(ua), ...CUA↓(uacagcag), and ...CUA↓(uacagcagagcagaaccaga). (C) Plot of the kinetic data for the three tail lengths. $k_{obs}$ values: 2-nt tail, 0.24 $min^{-1}$; 8-nt tail, 0.16 $min^{-1}$; 20-nt tail, 0.12 $min^{-1}$. For similar experiments with 9F21, see Supporting Information. For both 9F7 and 9F21, the $k_{obs}$ and ligation yield for a one-nucleotide 3′-tail were comparable to those with a two-nucleotide tail (data not shown).

are acceptable further away from the ligation junction (Figure 6). The 3′-tail of the left-hand substrate should be ≥1 nt in length for the highest ligation rates (Figure 8), but even linear 2′−5′ RNA (Figure 7) may be formed in good yield.

*Use of Deoxyribozymes for Preparative 2′,5′-Branch Formation.* The nanomole scale of the preparative ligation reaction shown in Figure 9 is consistent with the amount of RNA needed for many biochemical experiments. For example, nanomoles or less of RNA are required for both equilibrium and stopped-flow fluorescence folding assays (*35*−*38*). Of course, many common techniques (e.g., nondenaturing gel electrophoresis) require merely *pico*mole amounts of $^{32}$P-radiolabeled RNAs, and 9F7 should be particularly useful in those cases, even if the necessary RNA

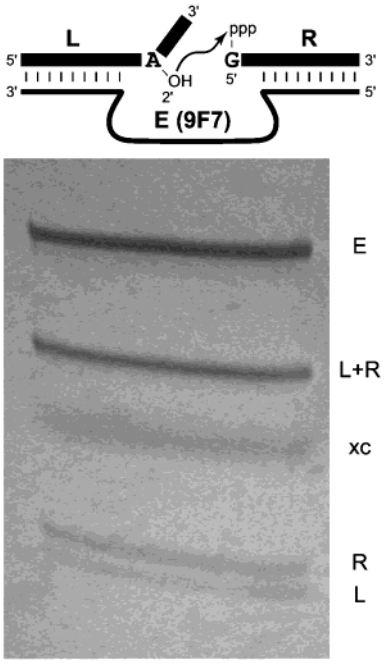


FIGURE 9: Nanomole scale preparative branch formation with 9F7. A 2.0 nmol scale reaction was performed using 2.0 nmol of left-hand RNA substrate L ...UA↓(uc) prepared by solid-phase synthesis, 2.2 nmol of 9F7 deoxyribozyme (E), and 2.4 nmol of right-hand RNA substrate R (200 μL total volume; 10−12 μM each nucleic acid). Incubation conditions were 50 mM HEPES, pH 7.5, 150 mM NaCl, 2 mM KCl, and 20 mM $MnCl_2$ at 37 °C for 30 min. The image was recorded while using a hand-held UV light to shadow the 3 mm thick 8% polyacrylamide gel placed over a fluorescent TLC plate (xc = xylene cyanol loading dye). After separate crush-and-soak extractions of the product L + R, the DNA enzyme E, and the unreacted substrate L, these were precipitated and quantitated by UV absorbance ($A_{260}$). The amounts of isolated material were as follows: 1.01 nmol of L + R (50% yield), 1.69 nmol of E (77% recovery), and 0.29 nmol of L (15% recovery).

sequences are suboptimal for ligation. On the other hand, for material-intensive X-ray crystallography and NMR spectroscopy experiments, larger amounts than nanomoles are generally required, but there does not appear to be any particular barrier to obtaining these quantities of material using deoxyribozymes (note that the 1.0 nmol of 2′,5′-branched RNA product in Figure 9 was obtained in just 200 μL of reaction volume). The principal difficulties associated with scaling up are the separation and purification of large quantities of RNA. In addition to conventional denaturing PAGE on large scale, appropriate methods for this task have been described (for example, ref *39*).

*Deoxyribozymes for General Synthesis of Branched RNA Sequences.* The results with attempted ligation of the bI1 and ai5γ group II intron substrates indicate that 9F7 is applicable only when the right-hand RNA substrate is at most one nucleotide different from the 9F7 requirement ↓GRMWR. It should be noted that the left-hand and right-hand substrates used during the selection of 9F7 and 9F21 (...CUAUA and GGAAG..., respectively) were chosen arbitrarily and not for any relationship to naturally occurring branched RNAs. We therefore anticipate that selection of RNA ligase deoxyribozymes using RNA substrates specifically chosen to correspond to natural splicing-related sequences should provide deoxyribozymes capable of creating natural branched RNAs efficiently. Such targeted selections are in progress in our laboratory.

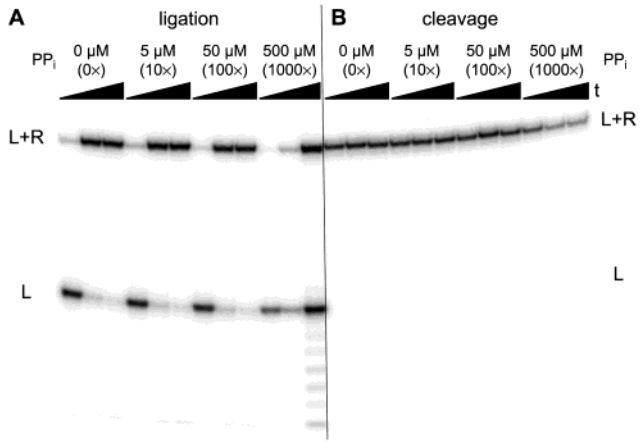


FIGURE 10: Effect of pyrophosphate ($PP_i$) on 9F7 ligation and cleavage. (A) 9F7-mediated ligation reactions in the presence of increasing concentrations of $PP_i$. The concentrations of L, E, and R were ~0.5, 1.5, and 3 $\mu$M, with [$PP_i$] at 0, 5, 50, or 500 $\mu$M. The ratio of $PP_i$ to L was therefore 0, 10, 100, or 1000 (0−1000×). The ligation reaction is unaffected except at the highest [$PP_i$], where the reaction is not complete at either 0.5 or 4 h. The standard incubation conditions were 50 mM HEPES, pH 7.5, 150 mM NaCl, 2 mM KCl, and 20 mM $MnCl_2$ at 37 °C. In 10 $\mu$L reactions, 2 $\mu$L aliquots were removed after 0, 0.5, and 4 h, quenched onto 8 $\mu$L of stop solution, and analyzed by denaturing PAGE. The increase in absolute signal intensity at the longest time point with 500 $\mu$M $PP_i$ is reproducible but not fully understood; we tentatively attribute this to precipitation at long incubation times. (B) Attempted $PP_i$-induced cleavage of the 9F7 ligation product. The concentration of the PAGE-purified 5′-$^{32}$P-radiolabeled ligation product (L + R) was ~0.5 $\mu$M, and the concentration of E was 1.5 $\mu$M. The [$PP_i$] was 0, 5, 50, or 500 $\mu$M, providing a ratio of $PP_i$ to ligation product of 0, 10, 100, or 1000 (0−1000×). No cleavage to form L is observed at any $PP_i$ concentration. At the highest [$PP_i$], some of the L + R signal intensity is lost (47% remains at 4 h), which we ascribe to hydrolysis of the 5′-$^{32}$P-radiolabel.

In the same selection that led to 9F7 and 9F21, we also identified 9F13 and 9F18, deoxyribozymes that create 2′,5′-branched RNA with a branch-site uridine nucleotide. This uridine is located one nucleotide to the 5′-side of the branch-site adenosine used by 9F7 and 9F21 (see Figure 1B). Natural branch-site nucleotides other than adenosine are rare, but they do occur (*10*), and 9F13 and 9F18 can be explored in the same manner as reported here for 9F7 and 9F21, although we have not yet performed these experiments. Whereas 9F7 and 9F21 strongly prefer a branch-site adenosine, they do in fact function to a significant degree with U, C, or G at the branch site (Figure 4). For certain applications, such as those in which only picomole (radiolabeling) quantities of the branched RNAs are needed, 9F7 or 9F21 could be used to prepare these products regardless of which branch-site nucleotide is desired.

With 9F7 and 9F21, we have not tested right-hand RNA substrates that have other than a 5′-triphosphate G. This is for the purely practical reason that in vitro transcription with T7 RNA polymerase always incorporates a 5′-triphosphate G, and therefore other 5′-triphosphate nucleotides are not readily introduced using this approach. Solid-phase approaches are known for preparing 5′-triphosphate RNAs in a general manner (*40*−*42*), but we have not applied such methods in this study. Fortunately, many interesting 2′,5′-branched RNAs are those in which the 5′-linked nucleotide is in fact G, because that is the natural nucleotide at the 5′-splice site of most introns (*10*).

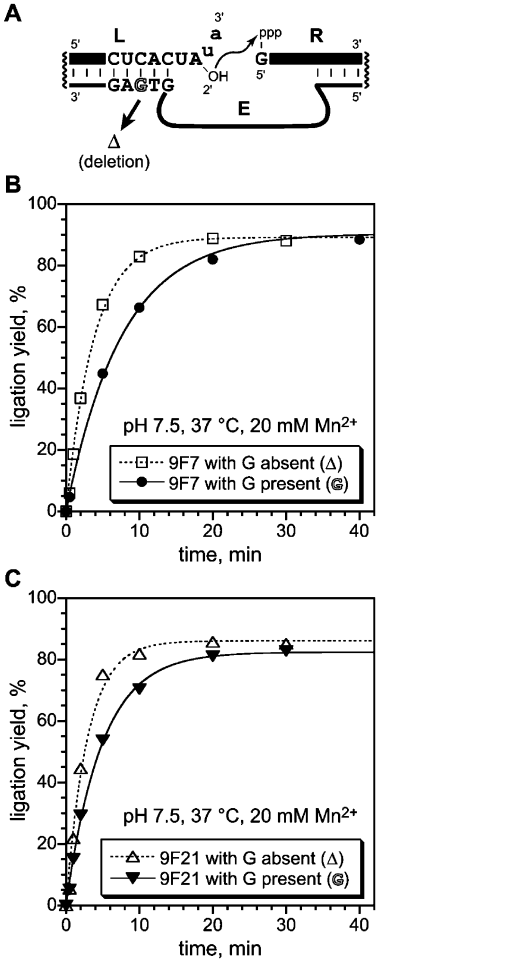


FIGURE 11: A deleted DNA nucleotide is preferred in the 9F7 and 9F21 binding arm. (A) Location of the deleted G nucleotide within the left-hand DNA binding arm. For the complete nucleotide sequences of the RNA and DNA, see the Experimental Procedures. (B) Ligation kinetics for 9F7 both with and without the indicated G nucleotide. $k_{obs}$ values: 9F7 with G absent (unpaired RNA nucleotide in L), 0.26 $min^{-1}$; 9F7 with G present, 0.13 $min^{-1}$. The left-hand substrate was ...UA↓(uc) prepared by solid-phase synthesis. (C) Ligation kinetics for 9F21 both with and without the indicated G nucleotide. $k_{obs}$ values: 9F21 with G absent (unpaired RNA nucleotide in L), 0.34 $min^{-1}$; 9F21 with G present, 0.20 $min^{-1}$. The left-hand substrate was ...UA↓(uc) prepared by solid-phase synthesis.

*Mechanism of Branch Formation.* Although we have no direct evidence for mechanisms to explain how 9F7 and 9F21 function, several indirect conclusions may be drawn from our findings. It is curious that $Mn^{2+}$ is much more effective as a cofactor than $Mg^{2+}$ (Figure 2), although only $Mg^{2+}$ was used during the selection procedure itself (*9*). This suggests that 9F7 and 9F21 have at least one metal binding site that specifically favors $Mn^{2+}$ over $Mg^{2+}$. The log-linear pH dependence (Figure 3) suggests that a single acidic site is deprotonated during branch formation, although the nature of this site is not known. The complicated right-hand RNA substrate requirement ↓GRMWR (Figure 5) suggests interesting tertiary structure contacts between 9F7 and its RNA substrate at these nucleotides. The observation that a zero tail length reduces the ligation rate 2 orders of magnitude (Figure 7) implies that the DNA nucleotides of 9F7 interact with the RNA 3′-tail nucleotides near the ligation junction. Conversely, the near-independence of ligation rate on tail length ≥2 nt (Figure 8) indicates that the deoxyribozyme

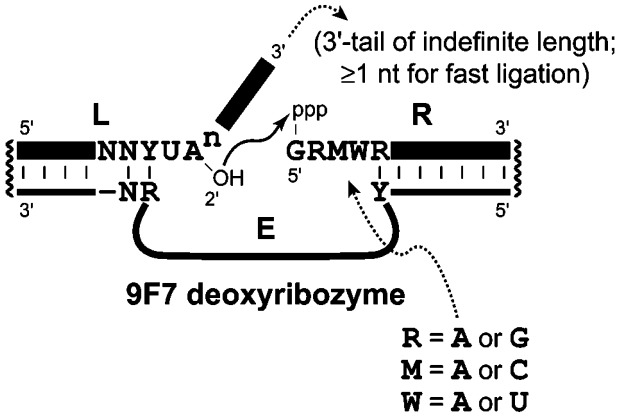


FIGURE 12: Summary of the sequence requirements for the 9F7 deoxyribozyme when used to synthesize 2′,5′-branched RNA. The ligation junction sequence requirements are derived from the data in Figures 5 and 6. The Y in the left-hand RNA substrate (L) is either C or U; the corresponding DNA nucleotide is the Watson−Crick purine complement. The N−N in the left-hand binding arm denotes any RNA−DNA Watson−Crick base pair. The adjacent N in the left-hand RNA substrate is unpaired for optimal activity (i.e., the corresponding DNA nucleotide is deleted; Figure 11). The 3′-tail of L should have at least one nucleotide as illustrated for the highest ligation rates (Figure 8), although even linear 2′−5′ RNA (with zero nucleotides in the 3′-tail) is synthesized in good yield (Figure 7). The right-hand RNA substrate has the relatively complicated sequence preference shown, as derived from the data in Figure 5. See Figure 1B for the 9F7 DNA sequence. The RNA−DNA binding arms on either side of the enzyme region are typically made long enough such that $\Delta G° \geq 14$ kcal/mol as computed from published parameters (*44*).

does not interact with these more remote nucleotides. The finding that the leaving group pyrophosphate does not significantly inhibit the ligation reaction except when present in large excess (Figure 10) indicates that binding of $PP_i$ by the deoxyribozyme is not particularly important. Finally, the intriguing finding that a deleted DNA nucleotide is preferred in the left-hand binding arm (Figure 11) suggests that some interesting structural feature of the deoxyribozyme−substrate complex is found near the ligation junction. Beyond these indirect inferences, direct structural information is needed for a full understanding of mechanism, and efforts along these lines are in progress.

In our preliminary report (*9*), we determined that the background reaction rate $k_{bkgd}$ for ligation of the left-hand and right-hand RNA substrates is $4 \times 10^{-7}$ min$^{-1}$ at 20 mM $Mn^{2+}$ versus $k_{obs} = 0.27$ min$^{-1}$ for 9F7-mediated ligation under the same conditions (0.13 min$^{-1}$ for 9F21). Therefore, the rate enhancement $k_{obs}/k_{bkgd}$ is at least $7 \times 10^5$ for 9F7 ($3 \times 10^5$ for 9F21), which further indicates that these DNA enzymes are worthy of mechanistic study. We anticipate that ongoing structural and biochemical investigations will help us to understand the mechanisms of 9F7 and 9F21 in greater detail.

## SUPPORTING INFORMATION AVAILABLE

Details of experiments not fully described in the text. This material is available free of charge via the Internet at http://pubs.acs.org.

## REFERENCES

1. Breaker, R. R. (1997) DNA enzymes, *Nat. Biotechnol. 15*, 427−431.
2. Breaker, R. R. (1997) In Vitro Selection of Catalytic Polynucleotides, *Chem. Rev. 97*, 371−390.
3. Breaker, R. R. (2000) Making catalytic DNAs, *Science 290*, 2095−2096.
4. Emilsson, G. M., and Breaker, R. R. (2002) Deoxyribozymes: new activities and new applications, *Cell. Mol. Life Sci. 59*, 596−607.
5. Wilson, D. S., and Szostak, J. W. (1999) In vitro selection of functional nucleic acids, *Annu. Rev. Biochem. 68*, 611−647.
6. Flynn-Charlebois, A., Wang, Y., Prior, T. K., Rashid, I., Hoadley, K. A., Coppins, R. L., Wolf, A. C., and Silverman, S. K. (2003) Deoxyribozymes with 2′-5′ RNA Ligase Activity, *J. Am. Chem. Soc. 125*, 2444−2454.
7. Flynn-Charlebois, A., Prior, T. K., Hoadley, K. A., and Silverman, S. K. (2003) In Vitro Evolution of an RNA-Cleaving DNA Enzyme into an RNA Ligase Switches the Selectivity from 3′-5′ to 2′-5′, *J. Am. Chem. Soc. 125*, 5346−5350.
8. Ricca, B. L., Wolf, A. C., and Silverman, S. K. (2003) Optimization and Generality of a Small Deoxyribozyme that Ligates RNA, *J. Mol. Biol. 330*, 1015−1025.
9. Wang, Y., and Silverman, S. K. (2003) Deoxyribozymes That Synthesize Branched and Lariat RNA, *J. Am. Chem. Soc. 125*, 6880−6881.
10. Burge, C. B., Tuschl, T., and Sharp, P. A. (1999) in *The RNA World* (Gesteland, R. F., Cech, T. R., and Atkins, J. F., Eds.) 2nd ed., pp 525−560, Cold Spring Harbor Laboratory Press, Cold Spring Harbor, NY.
11. Saldanha, R., Mohr, G., Belfort, M., and Lambowitz, A. M. (1993) Group I and group II introns, *FASEB J. 7*, 15−24.
12. Michel, F., and Ferat, J. L. (1995) Structure and activities of group II introns, *Annu. Rev. Biochem. 64*, 435−461.
13. Jacquier, A. (1996) Group II introns: elaborate ribozymes, *Biochimie 78*, 474−487.
14. Michel, F., Umesono, K., and Ozeki, H. (1989) Comparative and functional anatomy of group II catalytic introns−a review, *Gene 82*, 5−30.
15. Liu, Q., Green, J. B., Khodadadi, A., Haeberli, P., Beigelman, L., and Pyle, A. M. (1997) Branch-site selection in a group II intron mediated by active recognition of the adenine amino group and steric exclusion of nonadenine functionalities, *J. Mol. Biol. 267*, 163−171.
16. Nam, K., Hudson, R. H., Chapman, K. B., Ganeshan, K., Damha, M. J., and Boeke, J. D. (1994) Yeast lariat debranching enzyme. Substrate and sequence specificity, *J. Biol. Chem. 269*, 20613−20621.
17. Ooi, S. L., Dann, C., III, Nam, K., Leahy, D. J., Damha, M. J., and Boeke, J. D. (2001) RNA lariat debranching enzyme, *Methods Enzymol. 342*, 233−248.
18. Dahm, S. C., Derrick, W. B., and Uhlenbeck, O. C. (1993) Evidence for the role of solvated metal hydroxide in the hammerhead cleavage mechanism, *Biochemistry 32*, 13040−13045.
19. Pan, T., Dichtl, B., and Uhlenbeck, O. C. (1994) Properties of an in vitro selected $Pb^{2+}$ cleavage motif, *Biochemistry 33*, 9561−9565.
20. Santoro, S. W., and Joyce, G. F. (1998) Mechanism and utility of an RNA-cleaving DNA enzyme, *Biochemistry 37*, 13330−13342.
21. Suga, H., Cowan, J. A., and Szostak, J. W. (1998) Unusual metal ion catalysis in an acyl-transferase ribozyme, *Biochemistry 37*, 10118−10125.
22. Ota, N., Warashina, M., Hirano, K., Hatanaka, K., and Taira, K. (1998) Effects of helical structures formed by the binding arms of DNAzymes and their substrates on catalytic activity, *Nucleic Acids Res. 26*, 3385−3391.
23. Bergman, N. H., Johnston, W. K., and Bartel, D. P. (2000) Kinetic framework for ligation by an efficient RNA ligase ribozyme, *Biochemistry 39*, 3115−3123.
24. Li, J., Zheng, W., Kwon, A. H., and Lu, Y. (2000) In vitro selection and characterization of a highly efficient Zn(II)-dependent RNA-cleaving deoxyribozyme, *Nucleic Acids Res. 28*, 481−488.
25. Pyle, A. M., and Green, J. B. (1994) Building a kinetic framework for group II intron ribozyme activity: quantitation of interdomain binding and reaction rate, *Biochemistry 33*, 2716−2725.
26. Knitt, D. S., and Herschlag, D. (1996) pH dependencies of the *Tetrahymena* ribozyme reveal an unconventional origin of an apparent $pK_a$, *Biochemistry 35*, 1560−1570.
27. Schmelzer, C., Schmidt, C., May, K., and Schweyen, R. J. (1983) Determination of functional domains in intron bI1 of yeast mitochondrial RNA by studies of mitochondrial mutations and a nuclear suppressor, *EMBO J. 2*, 2047−2052.

28. Hertweck, M., and Mueller, M. W. (2001) Mapping divalent metal ion binding sites in a group II intron by $Mn^{2+}$- and $Zn^{2+}$-induced site-specific RNA cleavage, *Eur. J. Biochem. 268*, 4610−4620.
29. Bonitz, S. G., Coruzzi, G., Thalenfeld, B. E., Tzagoloff, A., and Macino, G. (1980) Assembly of the mitochondrial membrane system. Structure and nucleotide sequence of the gene coding for subunit 1 of yeast cytochrome oxidase, *J. Biol. Chem. 255*, 11927−11941.
30. Peebles, C. L., Perlman, P. S., Mecklenburg, K. L., Petrillo, M. L., Tabor, J. H., Jarrell, K. A., and Cheng, H. L. (1986) A self-splicing RNA excises an intron lariat, *Cell 44*, 213−223.
31. Jacquier, A., and Michel, F. (1987) Multiple exon-binding sites in class II self-splicing introns, *Cell 50*, 17−29.
32. Jarrell, K. A., Peebles, C. L., Dietrich, R. C., Romiti, S. L., and Perlman, P. S. (1988) Group II intron self-splicing. Alternative reaction conditions yield novel products, *J. Biol. Chem. 263*, 3432−3439.
33. Daniels, D. L., Michels, W. J., Jr., and Pyle, A. M. (1996) Two competing pathways for self-splicing by group II introns: a quantitative analysis of in vitro reaction rates and products, *J. Mol. Biol. 256*, 31−49.
34. Fedorova, O., Su, L. J., and Pyle, A. M. (2002) Group II introns: highly specific endonucleases with modular structures and diverse catalytic functions, *Methods 28*, 323−335.
35. Silverman, S. K., and Cech, T. R. (1999) RNA Tertiary Folding Monitored by Fluorescence of Covalently Attached Pyrene, *Biochemistry 38*, 14224−14237.
36. Silverman, S. K., Deras, M. L., Woodson, S. A., Scaringe, S. A., and Cech, T. R. (2000) Multiple Folding Pathways for the P4−P6 RNA Domain, *Biochemistry 39*, 12465−12475.
37. Silverman, S. K., and Cech, T. R. (2001) An Early Transition State for Folding of the P4−P6 RNA Domain, *RNA 7*, 161−166.
38. Young, B. T., and Silverman, S. K. (2002) The GAAA tetraloop-receptor interaction contributes differentially to folding thermodynamics and kinetics for the P4−P6 RNA domain, *Biochemistry 41*, 12271−12276.
39. Nguyen, T. H., Cunningham, L. A., Hammond, K. M., and Lu, Y. (1999) High-resolution preparative-scale purification of RNA using the Prep Cell, *Anal. Biochem. 269*, 216−218.
40. Ludwig, J., and Eckstein, F. (1989) Rapid and Efficient Synthesis of Nucleoside 5′-*O*-(1-Thiotriphosphates), 5′-Triphosphates and 2′,3′-Cyclophosphorothioates Using 2-Chloro-4*H*-1,3,2-benzodioxaphosphorin-4-one, *J. Org. Chem. 54*, 631−635.
41. Gaur, R. K., Sproat, B. S., and Krupp, G. (1992) Novel Solid-Phase Synthesis of 2′-*O*-methylribonucleoside 5′-Triphosphates and Their α-Thio Analogues, *Tetrahedron Lett. 33*, 3301−3304.
42. Brownlee, G. G., Fodor, E., Pritlove, D. C., Gould, K. G., and Dalluge, J. J. (1995) Solid-phase synthesis of 5′-diphosphorylated oligoribonucleotides and their conversion to capped $m^7$Gppp-oligoribonucleotides for use as primers for influenza A virus RNA polymerase in vitro, *Nucleic Acids Res. 23*, 2641−2647.
43. Milligan, J. F., Groebe, D. R., Witherell, G. W., and Uhlenbeck, O. C. (1987) Oligoribonucleotide synthesis using T7 RNA polymerase and synthetic DNA templates, *Nucleic Acids Res. 15*, 8783−8798.
44. Sugimoto, N., Nakano, S., Katoh, M., Matsumura, A., Nakamuta, H., Ohmichi, T., Yoneyama, M., and Sasaki, M. (1995) Thermodynamic parameters to predict stability of RNA/DNA hybrid duplexes, *Biochemistry 34*, 11211−11216.

BI0355847